

Solar Flare Effect to Sq Variation of Geomagnetic Field Observed at Biak Station from 1992 to 2003

Visca Wellyanita¹, La Ode Muhammad Musafar², Ahmad Zulfiana Utama¹, Mira Juangsih¹, Siska Filawati¹, Rizal Suryana¹, Setyanto Cahyo Pranoto¹, Yana Robiana¹, Refina Sri Fitri Wisnu³

¹Research Center for Space, National Research and Innovation Agency - BRIN, Indonesia

²Pontianak Observatory of Space and Atmosphere, National Research and Innovation Agency, Pontianak, Indonesia

³Department of Geophysics, Tanjungpura University, Pontianak, Indonesia
e-mail: visc001@brin.go.id

Received: 05-09-2023. Accepted: 02-08-2024. Published: 31-12-2024

Abstract

We analyzed the dependence of the geomagnetic Sq field variation at the Biak magnetic field observation station using data from a magnetometer from 1992 to 2003. The Biak station is a low magnetic latitude station, making the dominant variation of the magnetic field component that related to ionospheric currents representable by H-component. The Sq field was extracted from the magnetometer data using the 4th Harmonics Fourier decomposition method. This technique was applied to 1-hour average data of the H-component of the magnetic field. To investigate the dependence of the Sq field amplitude on solar flare events, we selected Sq field variations during flare events without magnetic storms. Additionally, before conducting the Fourier decomposition, we applied Dst index correction to the magnetic field variation data to eliminate the effects of magnetospheric currents. The study shows that Sq variation is highly correlated with X-class flares, which are the most energetic type of flares. Conversely, the lowest amplitude is linked to A-class flares with the lowest energy. These findings indicate that X-class flares generate Sq currents and induce the strongest magnetic fields compared to other classes of flares.

Keywords: Sq fi variation, geomagnetic strom, solar flares.

1. Introduction

The Sun continuously emits electromagnetic radiation across a wide range of wavelengths, from short wavelengths in the ultraviolet spectrum to long wavelengths in the infrared spectrum. The solar electromagnetic radiation flux increases when solar activity also increases. The solar activity is typically quantified using the sunspot number which is also known as the Wolf number (Clette et al., 2014; Cliver & Svalgaard, 2007). The sunspot number is derived from the number of sunspot groups which are distributed across the surface of the sun (Clette et al., 2007; Hathaway et al., 2002). Throughout a solar cycle, the sunspot number fluctuates, with higher values indicating stronger solar activity and a greater emission of electromagnetic radiation.

The sunspot is an active region on the surface of the sun with a stronger magnetic field than its surroundings (Thomas & Weiss, 2009; Lopez, et al., 2018). The magnetic field in these regions can be thousands of times stronger than the sun's average magnetic field. The sunspot groups are made up of spots that are connected by magnetic field lines in a closed configuration. This configuration is naturally unstable. This instability arises due to the sun's plasma nature and the relative motion of magnetic field lines with opposing polarities, causing them to draw closer or move farther apart. Consequently, the abundance of magnetic field lines with opposing polarities leads to magnetic reconnection (Tian et al., 2018; Luc et al., 2021), altering the sunspot group's configuration from closed to open. This process releases a substantial amount of energy, often culminating in solar flares and triggering subsequent solar activities. Large solar flares can discharge energy in the form of electromagnetic radiation, with peak flux exceeding 10^{-4} Watt/m², spanning wavelengths

from 0.1 to 0.8 nm. Solar flares are categorized into various classes based on the peak emitted electromagnetic radiation flux, denoted by A, B, C, M, and X classes.

Solar flares have consequences on Earth's response. Affecting both the magnetosphere and the ionosphere. The impact of solar flares on the Earth's magnetic field could be seen in H-component. During the solar flare events, there is an increase in H-component, particularly at high latitudes. However, H-component increment also occurred at equator but in lower value (Rastogi, et. al, 1999; Rastogi, 2001; Rastogi, 2003; Villante and Regi, 2008; Curto, 2020). Solar flares also influence geomagnetic pulsations with large periods (70 to 100 s) (Kato, et. al, 1959). In the Earth's ionosphere, solar flares enhance a dramatic ionization showed by Global Navigation Satellite System (GNSS), which Total Electron Content (TEC) increase by 30% in five minutes (Liu, et. al, 2021).

When solar radiation reaches the earth's atmosphere, the dayside of the atmosphere absorbs radiation in various ranges of the electromagnetic spectrum, resulting in an elevated temperature of the upper atmosphere. When the thermal energy becomes sufficiently high or surpasses the binding energy of atoms or molecules, it initiates ionization within the upper atmosphere. The upper atmosphere is composed of a mixture of neutral and ionized particles.

This process of daytime heating leads to temperature variations between day and night, generating upper atmospheric winds from regions of higher to lower temperatures. The neutral wind causes the movement of ionized particles within the upper atmosphere or the drift of charged particles through interactions with neutral particles, influenced by the Earth's geomagnetic field. As a result, an electric field and current are generated (Kindervatter & Teixeira, 2022). These electric currents flowing within the upper atmosphere are referred to as ionospheric currents. The strength and concentration of these currents depend on the number of ionized particles present, which is influenced by the amount of electromagnetic radiation energy coming from the sun.

The Sq geomagnetic field is a magnetic field variation associated with the flow of ionospheric current in the upper atmosphere (Matsushita & Maeda, 1965). The ionospheric current flow induces a secondary magnetic field and adds to the ambient geomagnetic field (Choudhary et al., 2011). The strength and fluctuation of ionospheric currents determine the induced field, and they are affected by the level of ionization in the upper atmosphere, which changes with local time. The dayside has a greater number of ionized particles compared to the night side. As a result, the ionospheric currents that flow on the dayside are stronger than those on the night side. Correspondingly, the induced field on the dayside is larger than that on the night side. In the low-latitude, measurements of the geomagnetic field show that the peak of the magnetic field variation occurs around noon of local time.

An increase in electromagnetic radiation during the flare induces a larger magnetic field. In this paper, we will examine the effect of solar flares on the geomagnetic Sq field measured by a station observing the earth's magnetic field at low latitudes, in this case the one observed at the Biak station, Indonesia.

2. Methodology

We analyzed the magnetic field variation observed at Biak station during the period from June 1992 to December 2002. Biak station is a low-latitude station where the geographical coordinate with (1.08°S; 136.1°E) and (12.2°S; 207.3°W) in the geomagnetic coordinate. The magnetometer at Biak recorded three components of magnetic field variation in the HDZ system for 11 years. The main field has been removed from the data. While H, D, and Z represent the components of the geomagnetic field in the north-south, east-west, and vertically downward, respectively. Additionally, the magnetometer captures a high-resolution magnetic field with 1-second time-sampling.

In this research, we analyzed the H-component of the magnetic field variation at Biak, which is a low-latitude station, and found that the Sq current dominantly flows eastward. We analyzed Sq variation in 1-hour resolution. The 1-second data is needed to check if the data contains noises that should be excluded from analyses. An example of the H-component of the magnetic field variation recorded at the Biak station is shown in Figure 1. The horizontal axis of the image represents the day of the month, while the vertical axis represents the H component of the magnetic field variation in nano-tesla.

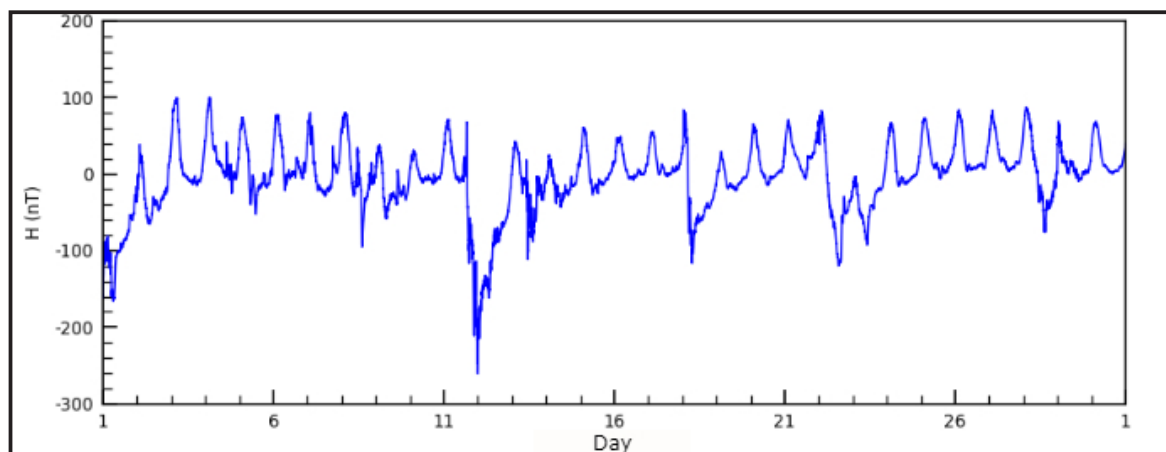
Table 1: Number of flare C and X during 1992-2003

| Year | A number of days solar flare event | | Flares associated with geomagnetic storms | |
|------|------------------------------------|----|---|----|
| | C | X | C | X |
| 1992 | 322 | 9 | 131 | 4 |
| 1993 | 232 | - | 97 | - |
| 1994 | 137 | - | 51 | - |
| 1995 | 65 | - | 18 | - |
| 1996 | 33 | 1 | 1 | - |
| 1997 | 102 | 3 | 26 | 1 |
| 1998 | 266 | 12 | 96 | 4 |
| 1999 | 326 | 4 | 86 | 1 |
| 2000 | 357 | 14 | 127 | 2 |
| 2001 | 342 | 17 | 108 | 12 |
| 2002 | 354 | 12 | 119 | 4 |
| 2003 | 286 | 14 | 124 | 10 |

The daily variation in the geomagnetic field on the ground comes from multiple sources. The presence of ring currents in the magnetosphere is one of the primary sources. The ring current is a diamagnetic current and becomes stronger when a magnetic storm occurs. It can change the pattern of the geomagnetic field so that the ionospheric current cannot maintain the daily magnetic variation. Therefore, the analysis of the Sq field in this paper was initiated by first reducing the impact of ring currents. The Dst index (Disturbance Storm Time index) is utilized to measure the manifestations of ring current strength that are present in the geomagnetic field. Yamazaki & Maute (2017) have conducted the reduction or elimination of the ring currents' effects, or Dst index correction, from the daily geomagnetic field data. To remove the ring current effect in H-component data is represented by:

$$H_{nt} = \alpha + \beta T_{nt} + \gamma Dst_{nt} \quad (2-1)$$

where Dst index represents a measurement of geomagnetic disturbances at low latitudes, T represents time in Julian day, and subscript nt was used to represent night-time data. This means Hnt that the measured H-components were selected for local night-time. The selection criterion assumes that the ionospheric current flow is considered being small during the local night-time. Therefore, the shifting in the H-component during this period can be considered from the contribution from ring current. Also, we analyzed α , β , and γ parameters by least square method.

**Figure 2-1:** Monthly H-component of magnetic variation at Biak station in April 2001

Prior to applying equation (2-1), the H-component uses 1-second resolution data. Whenever the noises were found in the data, they were excluded from the calculation of hourly averaged data. The hourly average of the H-component was performed to match its time resolution with Dst index. If the parameters of α , β , and γ are obtained from the corrected vari-

ation of the H-component, the daily variation resulting from the contribution of ring current can be derived for each hour of the day using equation (2-1). So, the corrected daily variations were calculated as the difference between the measured H-component and the reconstructed H-component from Dst index (ring-current) contribution, as follows:

$$H_{cor} = H_{meas} - (\alpha + \beta T_n + \gamma Dst_n) \quad (2-2)$$

where H_{meas} and H_{cor} represent measured and corrected H-components, respectively.

Sq field variations were calculated from corrected H-component by applying the Fourier decomposition method which was given by (Serov, 2017; Campbell, 2003),

$$H_{meas} = a_0 + \sum_{n=1}^{n=4} a_n \cos\left(\frac{2\pi n t}{24}\right) + \sum_{n=1}^{n=4} b_n \sin\left(\frac{2\pi n t}{24}\right) \quad (2-3)$$

where a_0 is a constant from averaged value of the periodic value, a_n and b_n represent Fourier coefficients and in this case, the highest harmonic number $n = 4$ has been chosen, t represents time in hour.

3. Result and Discussion

Yamazaki (2022) and Gu et al (2022) have been studying the diurnal and semi-diurnal variations of the geomagnetic field component for a considerable period. These two components are the main sources of daily variation of geomagnetic fields at low latitudes. The diurnal variation is affected by the amount of solar radiation that causes ionization of the upper atmosphere. The more ionized constituents of the upper atmosphere will cause stronger ionospheric current flowing which in turn will result in a larger induction magnetic field in addition to the earth's magnetic field.

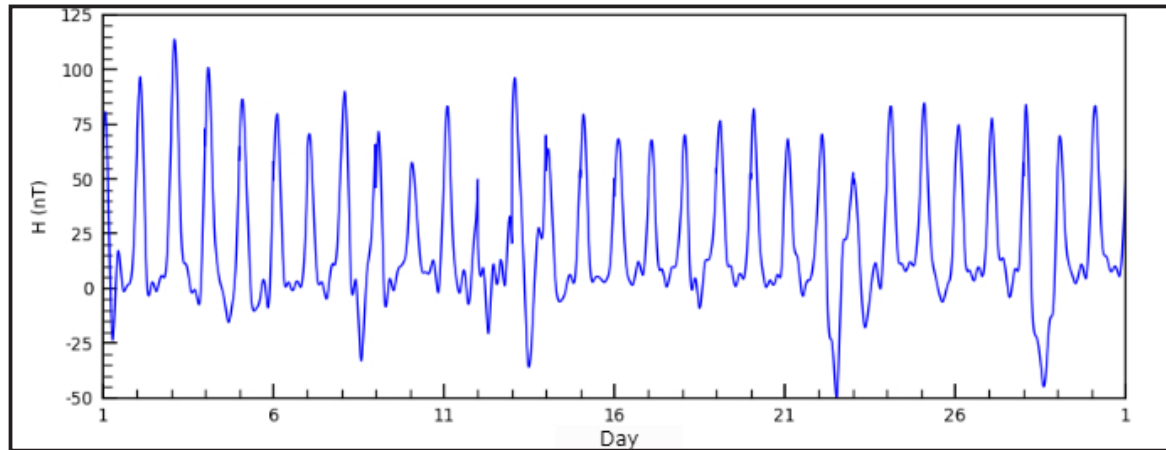


Figure 3-1: Corrected H-component for similar data set shown in Figure 2-1.

The data shown in Figure 2-1 contains both variations in geomagnetic quiet conditions and geomagnetic storms. As shown in Figure 2-1, a large geomagnetic storm occurred on the day of 12 shown in grey dash line, presenting a significant fluctuation in the geomagnetic field that dropped to a minimum peak of about 300 nano-tesla. During the geomagnetic storm, the geomagnetic field no longer shows diurnal variation due to the strong influence of the ring currents. Figure 3-1 depicts the application of the Dst index correction method discussed above and illustrates the results for the data shown in Figure 2-1. With applying (2-2), the corrected H-component shows the diurnal variation even during large magnetic storms. However, the magnetic variation is lower during a magnetic storm because the ionospheric Sq currents cannot maintain the weakening of the geomagnetic field caused by ring currents.

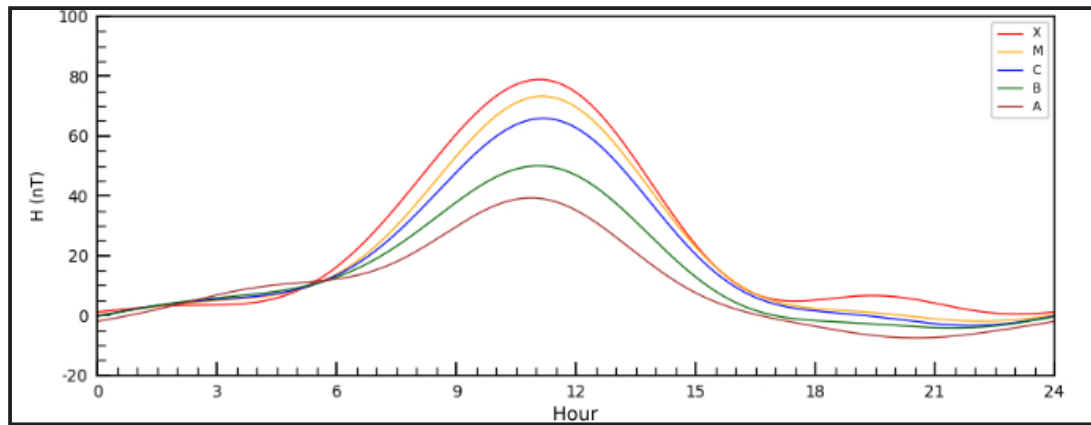


Figure 3-2: Comparison of average Sq variation derived from Biak data in various classes of flares.

While the Dst index correction does not completely remove the induced magnetic field caused by ring currents, this aspect requires further analysis after this paper. In this paper, we analyzed the geomagnetic data related to solar flares that were selected during periods when magnetic storms were not observed according to the Dst index. With this choice, we expected that the Sq field is obtained from the daily variation where the influence of ionospheric currents is dominant.

Figure 3-2 shows the average Sq field variation based on flare class, A to X. The flare classes in A, B, C, M, and X denote the maximum order of energy emitted during the flare event, respectively. A-class flares are the class of solar flares with the lowest emitted electromagnetic radiation energy, while X-class are the highest. Number of flare events that associated with analyzed Sq field are shown in Table 1. Figure 3-2 shows that the average Sq variation is highest when X-class flares occur, followed by Sq variations related to classes of M, C, and B-class flares and the lowest associated with A-class. This result is related to the theory that X-class flares emit energy. The strongest radiation will cause a higher ionospheric ionization rate compared to other classes and generate stronger electric currents and induce magnetic fields. Similarly, A-class flare emits lower electromagnetic radiation than other classes and produce the least ionization and the smallest induced magnetic field.

We also examined the Sq related to C-class and X-class flares as shown in Figure 3.3. The selection of flare events performed with manually checking of Dst index to ensure that there is no magnetic storm when the flare occurs. The gray-colored lines display the Sq variation during class C flare events, while the thick black line graph represents the average value. The orange-colored lines depict the Sq variation during class X flare events, and the thick red line graph represents the average value. Figure 3.3 shows that the variation of Sq and its average values during X- flares is greater than during C- flares.

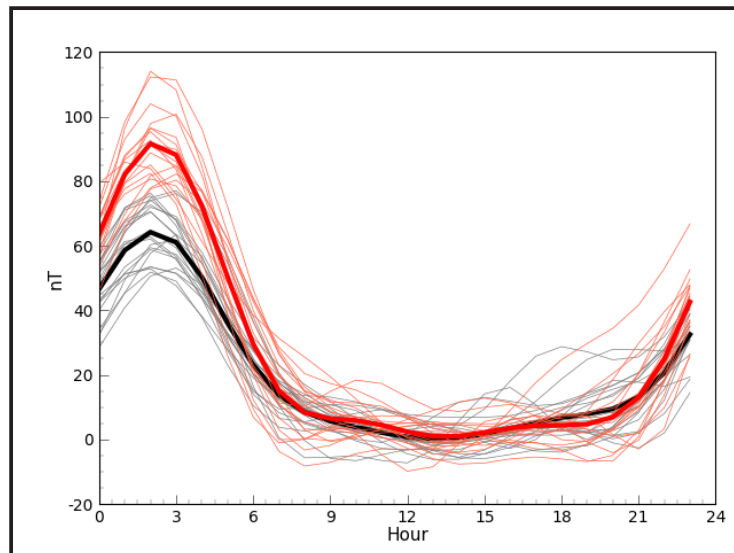


Figure 3-3: Comparison of Sq variation and its average values associated with magnetic storms derived from Biak data in C (gray and black lines) and X class flares (orange and red lines).

4. Conclusions

Sq variation derived from low-latitude geomagnetic field variation observed at Biak station for the 1992-2022 period has been analyzed. The Sq variations were analyzed to be associated with the occurrence of solar flares. The analysis was carried out only for Sq variation during flare events and the day when there was no magnetic storm. The results show that the largest amplitude of Sq is associated with X-class flares which have the highest energy compared to other class flares, and the lowest amplitude is associated with A-class flares which have the lowest energy. This shows that the X-class flare with the greatest energy generates the current Sq and the induced larger magnetic field compared to other class flares.

Acknowledgements

The author would like to thank all members of Biak station who gave generously of their time to collect the data and maintain the magnetometer operation. The author also thanks Prof. Kiyohumi Yumoto who installed the magnetometer as a part of the Circum Pan Magnetometer Network under research collaboration of BRIN (formerly, LAPAN), Indonesia, and SERC, Japan. This study was funded by the National Research and Innovation Agency, Indonesia.

Contributorship Statement

VW and LMM conceived of the presented idea and main contributors of this paper. VW also contributed to data processing and preparation of the manuscript. LMM designed and developed software for data processing. AZU and SCP contributed to editing the manuscript. MJ and SF contributed to data quality checking and noise removal. RS contributed to data processing. YN and RSF contributed to data collecting.

References

- Angeli, D. (1999). Input-to-state stability of PD-controlled robotic systems. *Automatica*, 35(1999), 1285–1290. [https://doi.org/https://doi.org/10.1016/S0005-1098\(99\)00037-0](https://doi.org/https://doi.org/10.1016/S0005-1098(99)00037-0)
- Chaturvedi, N. A., Amit K. Sanyal, & N. Harris McClamroch. (2011). Rigid Body Attitude Control: Using Aschwanden, M.J., et al., 2017. Global Energetics of Solar Flares. V. Energy Closure in Flares and Coronal Mass Ejections, *The Astronomical Journal*, 836, 17.
- Campbell, W.H., 2003, Introduction to Geomagnetic Fields, 2nd Edition, Cambridge University Press.

- Choudhary, R.K. J.-P. St.-Maurice, K.M. Ambili, S. Sunda, B.M. Pathan, The Impact of The January 15, 2010, 2011. Annular Solar Eclipse on The Equatorial and Low Latitude Ionospheric Densities. *Journal of Geophysical Research*, 116, A09309.
- Clette, F. D. Berghmans, P. Vanlommel, R.A.M. Van Der Linden, A. Koeckelenbergh, L. Wauters, 2007. From The Wolf Number to the International Sunspot Index: 25 Years of Sidc. *Adv. Space Res.* 40, 919–928.
- Clette, F. L. Svalgaard, J.M. Vaquero, E. W. Cliver, 2014. Revisiting The Sunspot Number: A 400-Year Perspective on the Solar Cycle, *Space Science Reviews*, 186, 35-104.
- Cliver, E.W., L. Svalgaard, 2007. In *Origins of The Wolf Sunspot Number Series: Geomagnetic Underpinning*, AGU Fall Meeting, Abstract Sh13a-1109.
- Fleishman, G.D., D.E. Gary, B. Chen, N. Kuroda, S. Yu, G.M. Nita, 2020. Decay of The Coronal Magnetic Field can Release Sufficient Energy to Power a Solar Flare, *Science*, 367, 6457.
- Gu, S-Y, J. Qi, C. Zhou, C. Yang, M. Jia, G. Li, B. Ning, X. Dou, 2020, Tidal Variations in The Ionosphere and Mesosphere Over Eastern China During 2014, *Journal of Geophysical Research: Space Physics*, 25:2.
- Hathaway, D.H., R.M. Wilson, E.J. Reichmann, 2002. Group Sunspot Numbers: Sunspot Cycle Characteristics. *Sol. Phys.* 211, 357–370.
- Kindervatter, T.H., F.L. Teixeira, 2022. *Tropospheric and Ionospheric Effects On Global Navigation Satellite Systems*, IEEE Press.
- Kato Y., Tamao T., Saito T., 1959. Geomagnetic pulsation accompanying the intense solar flare. *J Geomagn Geoelectr* 10: 203–207.
- Liu, J., Wang, W., Qian, L. et al., 2021. Solar flare effects in the Earth's magnetosphere. *Nat. Phys.* 17, 807–812.
- Lopez, K.F., V. S. Canedo, D. P. Cabezas, and Y. J. Buleje, 2018. Sunspot Characteristics of Active Regions NOAA 2268 and NOAA 2305. *IOP Conference Series, Journal of Physics: Conference Series*, 1143.
- Luc H.M., R. Van Der Voort, J. Joshi, V.M.J. Henriques, and S. Bose, 2021. Signatures of Ubiquitous Magnetic Reconnection in the Deep Atmosphere of Sunspot Penumbrae, *Astronomy & Astrophysics*, 646, A54.
- Matsushita, S., H. Maeda, 1965. On The Geomagnetic Solar Quiet Daily Variation Field During The Igy. *Journal of Geophysical Research*. 70, 2535–2558.
- Priest, E.R., 1991. The Magnetohydrodynamics of Energy Release in Solar Flares, *Philosophical Transactions of the Royal Society A: Mathematical, Physical and Engineering Sciences*, 336, 1643.
- Rastogi, R.G., Pathan B.M., Rao D.R.K., Sastry T.S., Sastri J.H., 1999. Solar flare effects on the geomagnetic elements during normal and counter electrojet periods. *Earth Planets Space* 51(947–957).
- Rastogi R.G., 2001. Electromagnetic induction due to solar flares at equatorial stations. *J Atmos Sol-Terr Phys* 63: 599.
- Rastogi R.G., 2003. Effect of a solar disturbances on the geomagnetic H, Y and Z fields in American equatorial electrojet stations: Solar flare effects. *J Ind Geophys Union* 7(2): 43.
- Serov, V., *Fourier Series, Fourier Transform and their Application to Mathematical Physics*, Springer, Pp. 11-13, 2017
- Thomas, J.H. and N.O. Weiss, 2009, *Sunspots and Active Regions in Sunspot and Starspots*,

Cambridge Univerisity Press.

- Tian, H., V. Yurchyshyn, H. Peter, S.K. Solanki, P.R. Young, L. Ni, W. Cao, K. Ji, Y. Zhu, J. Zhang. 2018. Frequently Occurring Reconnection Jets from Sunspot Light Bridges, *The Astronomical Journal*, 854, 92.
- Villante U., Regi M., 2008. Solar flare effect preceding Halloween storm (28 October 2003): Results of a worldwide analysis. *J Geophys Res* 113: A00A05.
- Yamazaki, Y., Dan A. Maute, 2017. Sq and Eej- A Review of the Daily Variation of Geomagnetic Field Caused by Ionospheric Dynamo Currents, *Space Science Reviews*, 206:299-405.
- Yamazaki, Y., 2022, Solar and Lunar Daily Geomagnetic Variations and Their Equivalent Current Systems Observed by SWARM. *Earth, Planet and Space*, 74:99.
- Rotation Matricies for Continuous, Singularity-free Control Laws. *IEEE Control Systems Magazine*, 31(3), 30–51. <https://doi.org/10.1109/MCS.2011.940459>
- Hughes, P. . C. (2004). *Spacecraft Attitude Dynamics*. Dover Publications, Inc.
- LAPAN. (2021). LAPAN-A3 Satellite. Retrieved February 2, 2021, from <http://pusteksat.lapan.go.id/>
- Millan, R. M., von Steiger, R., Ariel, M., Bartalev, S., Borgeaud, M., Campagnola, S., ... Wu, J. (2019). Small Satellites for Space Science. *Advances in Space Research*. <https://doi.org/10.1016/j.asr.2019.07.035>